



η and η' mesons in nuclear matter and nucleiJ. J. Cobos-Martínez ^{1,*} and Kazuo Tsushima ²¹*Departamento de Física, Universidad de Sonora, Boulevard Luis Encinas J. y Rosales, Colonia Centro, Hermosillo, Sonora 83000, México*²*Laboratório de Física Teórica e Computacional-LFTC, Universidade Cidade de São Paulo, 01506-000 São Paulo, SP, Brazil*

(Received 17 August 2023; accepted 5 January 2024; published 12 February 2024)

We present updated and extended results for the η - and η' -nucleus bound state energies, obtained by solving the Schrödinger and Klein-Gordon equations with complex optical potentials, for a wide range of nuclei. The η and η' nuclear potentials are obtained in the local density approximation from the mass shift of these mesons in nuclear matter, which is calculated within the quark-meson coupling model. Our results show that the η and η' mesons are expected to form mesic nuclei with all the nuclei considered. However, the signal for the formation of the η - and η' -mesic nuclei may be difficult to identify experimentally due to possible large widths.

DOI: [10.1103/PhysRevC.109.025202](https://doi.org/10.1103/PhysRevC.109.025202)**I. INTRODUCTION**

The investigation of how the properties and structure of hadrons, such as masses and widths, are modified in a nuclear medium is one of the most exciting and important problems in hadron and nuclear physics, since these are connected to, for example, chiral symmetry restoration and the structure of the QCD vacuum [1], which in turn are reflected on the properties of hadrons in medium [2,3].

In particular, research on the η - and η' -meson masses and widths in nuclear matter and nuclei has received considerable interest in recent years since it is expected to give insight on the partial restoration of chiral symmetry at finite density, on the low-energy dynamics of QCD, which is related to the $U(1)_A$ anomaly, and on the formation of mesic bound states with nuclei—the so-called mesic nuclei; see Refs. [4–8] for recent reviews. Seen the other way around, the discovery of η - and η' -mesic nuclei would allow for a more accurate determination of the poorly known ηN and $\eta' N$ interactions, would open up opportunities to study the structure of these mesons in a nuclear medium [9], and provide information on the dynamics of the axial $U(1)_A$ anomaly in the nuclear medium [10].

The concept of mesic nuclei was first introduced by Haider and Liu in Ref. [11]. Mesic nuclei would represent a novel form of nuclear system in which a meson is bound with a nucleus only through the strong interaction, without the influence of electromagnetic Coulomb effects—such a bound state system by the Coulomb interaction is often called a “mesic atom.” The η and η' mesons are particularly promising candidates for exploring such meson-nucleus bound states [3].

The experimental searches for this exotic form of nuclear system involve the production of η and η' mesons, analyzing their interaction with nuclei, and detecting η - and η' -mesic states through their possible decay modes [4–8]. Despite more

than three decades of intense experimental efforts, unambiguous signals for the η - and η' -nucleus bound states have so far not been directly observed. However, experimental information on the strength of the η and η' meson interactions with nuclei has been extracted indirectly from a combination of measurements (production cross sections, transparency ratios, excitation functions, and momentum distributions in hadron- and photo-induced reactions) and Glauber-, transport-, or collisional-model approaches [4,5]. In this way the real and imaginary parts of the η -nucleus optical potential at normal nuclear density ρ_0 have been constrained to $|V_0| \lesssim 60$ MeV and $|W_0| \lesssim 7$ MeV, respectively, using the light nuclei ^4He [12,13]. Similar analyses have been applied to the η' -nucleus interaction, giving $V_0 \approx -40$ MeV [14–16] and $W_0 \approx -13$ MeV [3,17,18], using medium and heavy nuclei (C, Nb, and Pb). A more detailed discussion of the experimental efforts is given in Refs. [4–8]. Even though in both cases we have an attractive meson-nucleus interaction and a relatively weak meson absorption, as mentioned above, η - and η' -nucleus bound states have so far not been directly observed [19–21], and thus the search for this novel form of nuclear system continues [4–8].

On the theoretical side, the medium modifications of the η and η' mesons and their nuclear bound states have been studied in a variety of approaches, such as the quark-meson coupling (QMC) model [9,22], chiral coupled channels [23], the Nambu–Jona-Lasinio model [24–26], and linear σ model [27,28], and chiral unitary approach using a microscopic many-body theory [29,30], as well as other approaches [31,32]. The significant variation of input parameters in different calculations results in a wide range of predicted outcomes. Some of these theoretical analyses predict the existence of certain η - and η' -mesic nuclei; however, other suggest these are unlikely. See Refs. [4–8] for a more detailed discussion.

In this work we add to the existing theoretical efforts by updating and extending previous work [33,34] on the mass shift of the η and η' mesons in nuclear matter and their nuclear bound states using results obtained with the QMC model. The

*Corresponding author: jesus.cobos@unison.mx

approach followed here is an extension of previous work by us in Refs. [35–39]. Here we use an updated value for the pseudoscalar mixing angle of $\theta_p = -11.3^\circ$ from the Particle Data Group [40].

This paper is organized as follows. In Sec. II we briefly describe the QMC model and present results for the mass shift of the η and η' mesons in symmetric nuclear matter. Using the local density approximation, in Sec. III we compute potentials for the η and η' mesons in nuclei. In Sec. IV we present numerical results for the η - and η' -nucleus bound state energies by solving the Schrödinger and Klein-Gordon equations with the nuclear potentials calculated in Sec. III. By adding an imaginary part to the η - and η' -nucleus potentials, to simulate the absorption of these mesons by nuclei, in Sec. V we present our results for the single-particle energies and absorption widths for the η and η' in nuclei. Finally, in Sec. VI we conclude this work.

II. QUARK-MESON COUPLING MODEL: MASS SHIFT

In a nuclear medium, hadrons with light quarks, such as the η and η' mesons, are expected to change their properties, such as their masses, and thus affect their interaction with nucleons. In this section we will compute the mass shift of these mesons in nuclear matter using the quark-meson coupling model. In later sections we use these results to compute the η - and η' -nucleus potentials and single-particle energies.

The QMC model is a quark-based model for nuclear matter and finite nuclei that describes the internal structure of the nucleons using the Massachusetts Institute of Technology (MIT) bag model and the binding of nucleons by the self-consistent couplings of the confined light quarks u and d to the scalar- σ , vector-isoscalar- ω , and vector-isovector- ρ meson fields generated by the confined light quarks in the nucleons [41]. The QMC model has been successfully applied to investigate the properties of infinite nuclear matter and finite nuclei. Here we briefly present the necessary details needed to understand our results. For a more in-depth discussion of the model, see Refs. [42,43] and references therein.

We consider nuclear matter in its rest frame, where all the scalar and vector mean-field potentials, which are responsible for the nuclear many-body interactions, are constants in Hartree approximation. Assuming SU(2) symmetry for the quarks ($m_q = m_u = m_d$ and $q = u$ or d below), the Dirac equations for the quarks and antiquarks in nuclear matter, in a hadron bag $h = \eta, \eta'$ at the position $x = (t, \vec{r})$ (with $|\vec{r}| \leq R_h^*$, R_h^* being the in-medium bag radius), neglecting the Coulomb force, are given by [41–44]

$$[i\cancel{\partial}_x - (m_q - V_\sigma^q) \mp \gamma^0 V_+^q] \begin{pmatrix} \psi_u(x) \\ \psi_{\bar{u}}(x) \end{pmatrix} = 0, \quad (1)$$

$$[i\cancel{\partial}_x - (m_q - V_\sigma^q) \mp \gamma^0 V_-^q] \begin{pmatrix} \psi_d(x) \\ \psi_{\bar{d}}(x) \end{pmatrix} = 0, \quad (2)$$

$$[i\gamma \cdot \partial_x - m_s] \psi_{s,\bar{s}}(x) = 0. \quad (3)$$

Here $V_\pm^q = V_\omega^q \pm \frac{1}{2}V_\rho^q$; the (constant) mean-field potentials for the light quark q in nuclear matter are defined by $V_\sigma^q \equiv g_\sigma^q \sigma$, $V_\omega^q \equiv g_\omega^q \omega = g_\omega^q \delta^{\mu 0} \omega^\mu$, $V_\rho^q \equiv g_\rho^q b = g_\rho^q \delta^{i3} \delta^{\mu 0} \rho^{i,\mu}$, with the g_σ^q , g_ω^q , and g_ρ^q being the corresponding quark-meson

coupling constants. Note that $V_\rho^q \propto (\rho_p - \rho_n) = 0$ in symmetric nuclear matter, although this is not true in a nucleus where the Coulomb force may induce an asymmetry between the proton and neutron distributions, even in a nucleus with the same number of protons and neutrons, resulting in $V_\rho^q \neq 0$ at a given position in a nucleus. The static solution for the ground state quarks (antiquarks) with a flavor $f (= u, d, s)$ is written as $\psi_f(x) = N_f e^{-i\epsilon_f t/R_h^*} \psi_f(\mathbf{r})$, with the N_f being the normalization factor, and $\psi_f(\mathbf{r})$ the corresponding spin and spatial part of the wave function. The eigenenergies for the quarks and antiquarks in the η and η' mesons, in units of $1/R_{\eta,\eta'}^*$, are given by

$$\begin{pmatrix} \epsilon_u \\ \epsilon_{\bar{u}} \end{pmatrix} = \Omega_q^* \pm R_{\eta,\eta'}^* \left(V_\omega^q + \frac{1}{2} V_\rho^q \right), \quad (4)$$

$$\begin{pmatrix} \epsilon_d \\ \epsilon_{\bar{d}} \end{pmatrix} = \Omega_q^* \pm R_{\eta,\eta'}^* \left(V_\omega^q - \frac{1}{2} V_\rho^q \right), \quad (5)$$

$$\epsilon_s = \epsilon_{\bar{s}} = \Omega_s. \quad (6)$$

The in-medium mass m_h^* and bag radius R_h^* of hadron h are determined from

$$m_\eta^* = \frac{2[a_p^2 \Omega_q^* + b_p^2 \Omega_s] - z_\eta}{R_\eta^*} + \frac{4}{3} \pi R_\eta^{*3} B, \quad (7)$$

(for $\eta', \eta \rightarrow \eta'$, and $a_p \leftrightarrow b_p$),

$$\left. \frac{dm_h^*}{dR_j} \right|_{R_h=R_h^*} = 0, \quad (h = \eta, \eta'), \quad (8)$$

$$a_p \equiv \sqrt{1/3} \cos \theta_p - \sqrt{2/3} \sin \theta_p, \quad (9)$$

$$b_p \equiv \sqrt{2/3} \cos \theta_p + \sqrt{1/3} \sin \theta_p, \quad (10)$$

where $\Omega_q^* = \Omega_q^* = [x_q^2 + (R_{\eta,\eta'}^* m_q^*)^2]^{1/2}$, and $m_q^* = m_q - g_\sigma^q \sigma$ and $\Omega_s^* = \Omega_s^* = [x_s^2 + (R_{\eta,\eta'}^* m_s)^2]^{1/2}$, with $x_{q,s}$ being the lowest mode bag eigenfrequencies. B is the bag constant; $n_{q,s}$ ($n_{\bar{q},\bar{s}}$) are the lowest mode valence quark (antiquark) numbers for the quark flavors q and s in the corresponding η and η' mesons; and $z_{\eta,\eta'}$ parametrize the sum of the center-of-mass and gluon fluctuation effects and are assumed to be independent of density [45]. The MIT big parameters z_N (z_h) and B are fixed by fitting the nucleon (hadron) mass in free space.

We choose the values $(m_q, m_s) = (5, 250)$ MeV for the current quark masses, and $R_N = 0.8$ fm for the free space nucleon bag radius. (See Ref. [46] for the $(m_q, m_s) = (5, 93)$ MeV result.) The quark-meson coupling constants, g_σ^q , g_ω^q and g_ρ^q used for the light quarks in the η and η' mesons (the same as in the nucleon), were determined by the fit to the saturation energy (-15.7 MeV) at the saturation density ($\rho_0 = 0.15 \text{ fm}^{-3}$) of symmetric nuclear matter for g_σ^q and g_ω^q , and by the bulk symmetry energy (35 MeV) for g_ρ^q [41,42]. The obtained values for the quark-meson coupling constants are $(g_\sigma^q, g_\omega^q, g_\rho^q) = (5.69, 2.72, 9.33)$.

Finally, for the mixing angle θ_p we use the value $\theta_p = -11.3^\circ$, neglecting any possible mass dependence and imaginary parts [40,46]. Furthermore, we also assume that the value of the mixing angle does not change in the nuclear medium.

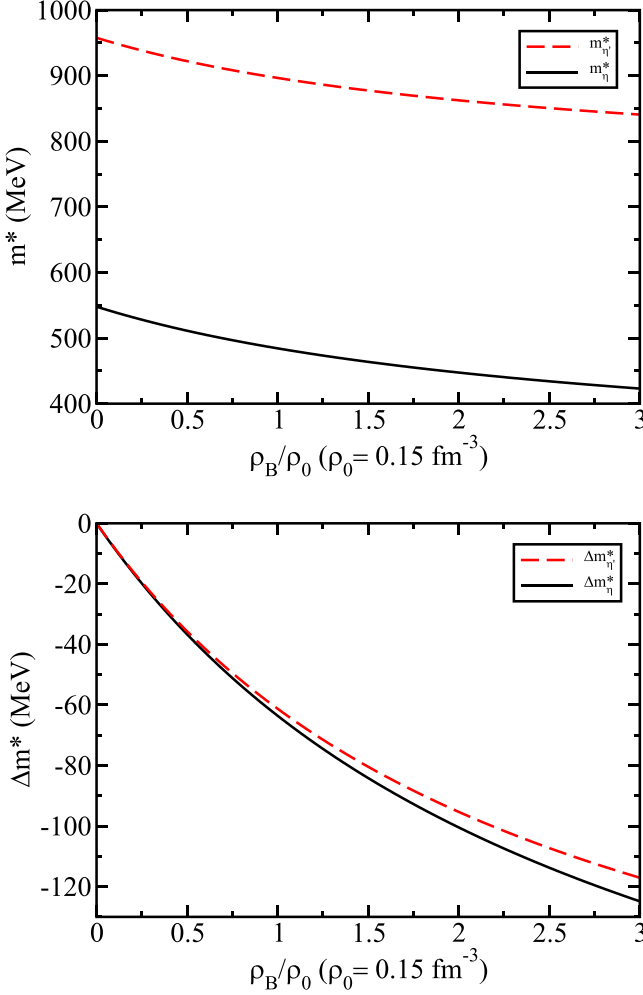


FIG. 1. η and η' masses (top panel) and mass shift (bottom panel) in nuclear matter calculated in the quark-meson coupling (QMC) model as a function of the nuclear matter density ρ_B .

In Fig. 1 we present the QMC model predictions for the masses and mass shift $\Delta m_h(\rho_B) \equiv m_h^*(\rho_B) - m_h$, where m_h^* is the in-medium meson mass and m_h is vacuum mass, for the η and η' mesons in symmetric nuclear matter as a function of the nuclear matter density ρ_B . Clearly, the masses of these mesons decrease in the nuclear medium, a clear signature of the partial restoration of chiral symmetry in the medium. The extracted values for the mass shift at nuclear matter saturation density is $\Delta m_\eta(\rho_0) = -63.6$ MeV and $\Delta m_{\eta'}(\rho_0) = -61.3$ MeV, respectively. These results are consistent with the values extracted for these quantities from experimental data, using transport, collision, or Glauber calculations of $V_0 = -60$ to 0 MeV for the η meson and $-40 \pm 6 \pm 15$ MeV for the η' meson [4,5].

Finally, in Fig. 2 we present results, for the first time, for the $U(1)_A$ mass $m_{U(1)_A} \equiv m_{\eta'}^2 + m_\eta^2 - 2m_K^2$ in nuclear matter, where $m_{\eta'}$, m_η , and m_K are the η , η' , and kaon masses in nuclear matter as a function of the nuclear matter density ρ_B , obtained in our approach. The $U(1)_A$ mass shift is related to the topological susceptibility and parametrizes the deviation from the $U(1)_A$ symmetric world [47]. Since $m_{U(1)_A} = 0$

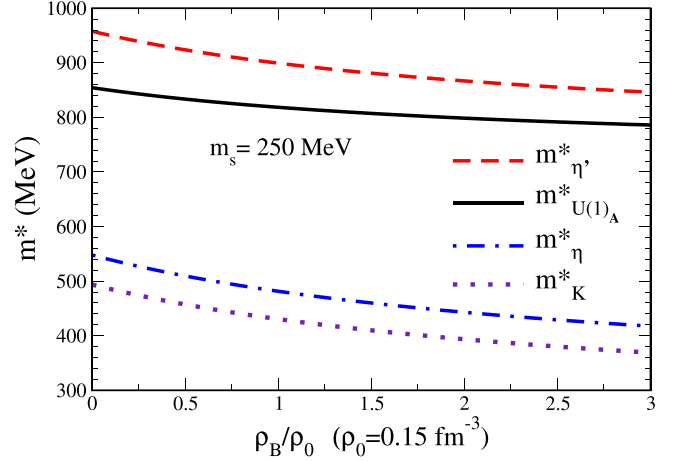


FIG. 2. $U(1)_A$ mass shift in nuclear matter calculated in the QMC model as a function of the nuclear matter density ρ_B .

means a $U(1)_A$ symmetric world, this result implies an effective partial restoration of the $U(1)_A$ symmetry in nuclear matter. However, a more complete study of the $U(1)_A$ symmetry in nuclear matter, in the approach followed in this work, deserves further investigation. At the moment there is no experimental information on the possible effective restoration of the $U(1)_A$ symmetry at finite density.

III. η - AND η' -NUCLEUS POTENTIALS

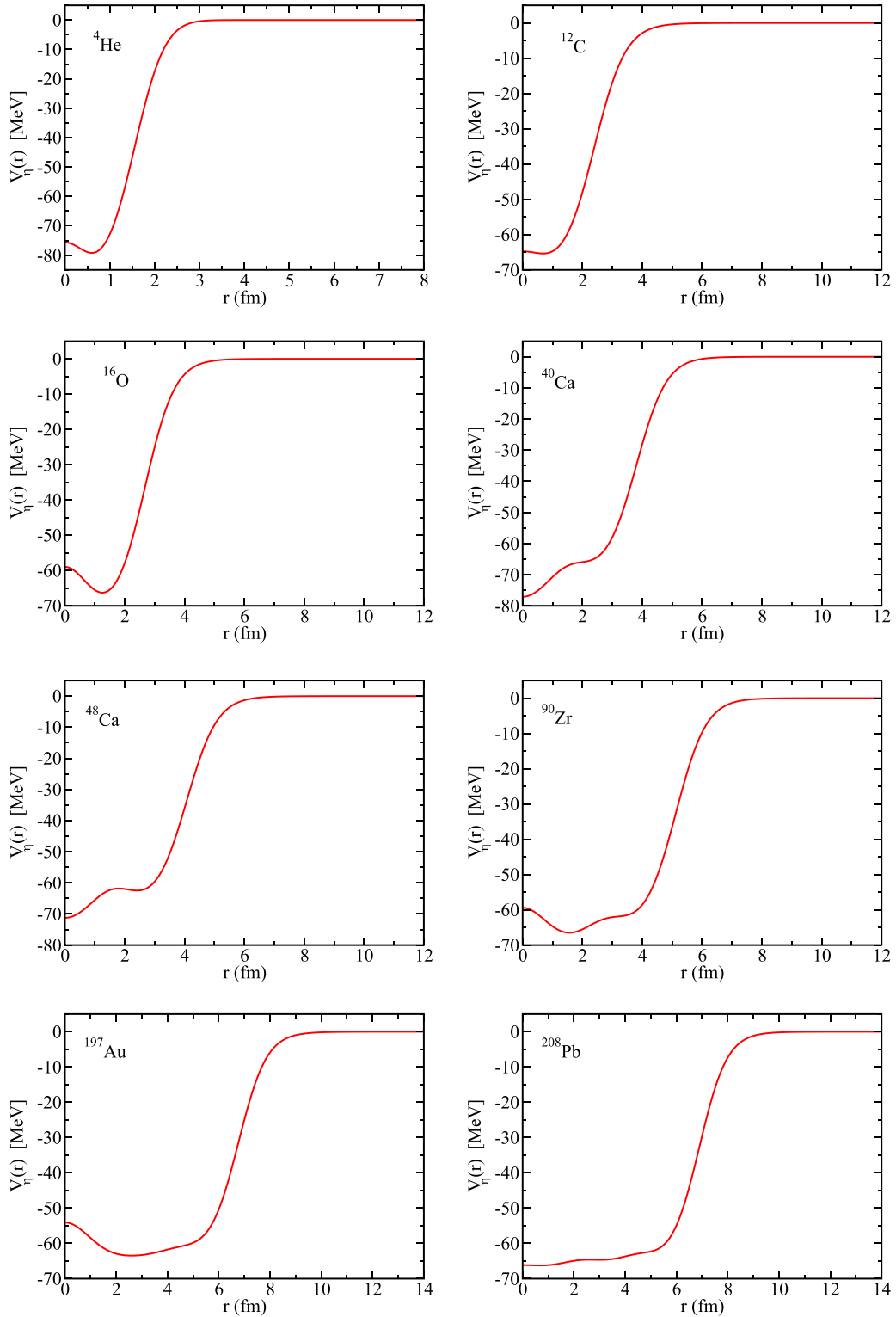
The mass shift for the η and η' in nuclear matter was calculated in the previous section as a function the nuclear matter density ρ_B using the QMC model, see Fig. 1. These results show that the nuclear medium provides attraction to these mesons and opens the possibility to study the binding of these mesons to nuclei, which we carry out in this section. First, we obtain the η and η' Lorentz scalar potentials in nuclei, and then we solve the Schrödinger and Klein-Gordon equations for these mesons using these potentials for various nuclei to obtain the η and η' single-particle energies of the η - and η' -nuclear bound states. We consider the situation in which these mesons have been produced nearly at rest inside a nucleus A and study the following nuclei in a wide range of masses, namely, ${}^4_2\text{He}$, ${}^{12}_6\text{C}$, ${}^{16}_8\text{O}$, ${}^{40}_{20}\text{Ca}$, ${}^{48}_{20}\text{Ca}$, ${}^{90}_{42}\text{Zr}$, and ${}^{208}_{82}\text{Pb}$.

The η and η' Lorentz scalar potentials in nuclei (no Lorentz vector potentials due to the $q\bar{q}$ structure) are calculated in the local density approximation

$$V_{hA}(r) = \Delta m_h(\rho_B^A(r)), \quad (11)$$

where $\Delta m_h(\rho_B) = m_h^*(\rho_B^A(r)) - m_h$ ($h = \eta, \eta'$) is the mass shift in nuclear matter as a function of the nuclear matter density ρ_B , $\rho_B^A(r)$ is the baryon density distribution of nucleons for a nucleus A , r is the distance from the center of the nucleus, and m_h is the mass of the meson in vacuum ($m_\eta = 547.862$ MeV and $m_{\eta'} = 957.78$ MeV)

The baryon density distributions for the nuclei listed above, that enter into Eq. (11), are calculated in the QMC model [48], except for ${}^4\text{He}$, which was parameterized in Ref. [49]. The calculated potentials for the η and η' mesons in nuclei

FIG. 3. η scalar potentials for several nuclei.

are shown in Figs. 3 and 4. These figures show that all potentials for the η and η' in nuclei are attractive. This is so because the corresponding mass shift (in nuclear matter) is negative for both mesons. The differences in the potentials, for a given meson, reflect the differences in the baryon density distributions for the nuclei studied. Furthermore, note

that for a given nucleus, the potentials for the η and η' are very similar, the reason for this being that \rightarrow similarity is because the mass shift for the η and η' is very similar, as shown in Fig. 1. To study the interactions of the η and η' with nuclei in more detail, we now consider the bound states of these mesons with nuclei when these mesons have been

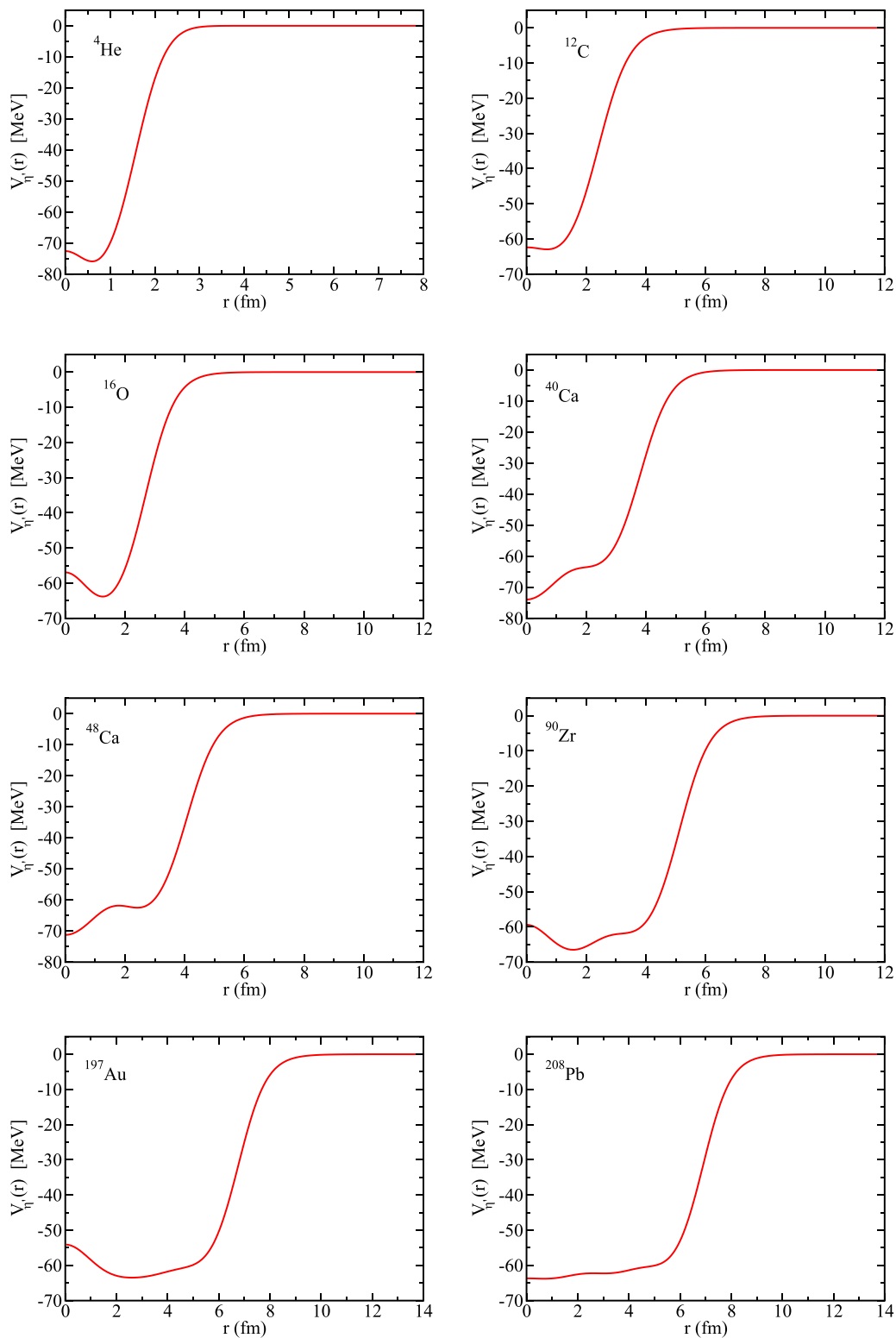


FIG. 4. η' scalar potentials for several nuclei.

produced inside a nucleus A and study the nuclear bound states, the so-called mesic nuclei, in a wide range of nuclear masses, namely, for the nuclei listed in the previous section.

IV. NUMERICAL RESULTS FOR THE η - AND η' -NUCLEUS BOUND STATE ENERGIES

In order to obtain the η and η' single-particle energies in nuclei and also to have an idea of the relativistic effects, we

TABLE I. Bound state energies (E) of the η meson in nucleus of mass number A obtained by solving the Schrödinger and Klein-Gordon equations. E is in MeV.

	$n\ell$	E (SE)	E (KGE)
${}^4_\eta\text{He}$	1s	-13.24	-10.99
${}^{12}_\eta\text{C}$	1s	-27.03	-25.25
	1p	-1.75	-0.87
${}^{16}_\eta\text{O}$	1s	-32.60	-30.78
	1p	-8.04	-6.47
${}^{40}_\eta\text{Ca}$	1s	-48.71	-46.93
	1p	-29.31	-26.93
	1d	-8.73	-6.67
	2s	-7.16	-5.43
${}^{48}_\eta\text{Ca}$	1s	-49.34	-47.78
	1p	-32.22	-29.97
	1d	-13.31	-11.08
	2s	-10.34	-8.7
${}^{90}_\eta\text{Zr}$	1s	-53.71	-52.56
	1p	-41.76	-39.85
	1d	-27.71	-25.32
	2s	-23.43	-21.04
${}^{197}_\eta\text{Au}$	1s	-55.85	-55.12
	1p	-48.45	-47.13
	1d	-39.48	-37.60
	2s	-36.04	-34.01
${}^{208}_\eta\text{Pb}$	1s	-57.59	-56.85
	1p	-50.27	-48.92
	1d	-41.40	-39.81
	2s	-38.03	-35.95

solve numerically the Schrödinger and Klein-Gordon equations for these mesons with the scalar nuclear potential given in Eq. (11) for various nuclei. We first solve the Schrödinger equation (SE),

$$\left(-\frac{1}{2m}\nabla^2 + V(\vec{r})\right)\psi(\vec{r}) = E\psi(\vec{r}), \quad (12)$$

where $V(\vec{r}) = V(r)$ is the scalar (nuclear) potential, given by Eq. (11), $r = |\vec{r}|$ is the distance from the center of the nucleus, and m is the reduced mass of the h -nucleus system in vacuum, with $h = \eta, \eta'$.

Next we solve the Klein-Gordon equation (KGE),

$$(-\nabla^2 + (m + V(\vec{r}))^2)\phi(\vec{r}) = \mathcal{E}^2\psi(\vec{r}), \quad (13)$$

where, as before, $V(\vec{r}) = V(r)$ is the scalar (nuclear) potential, given by Eq. (11), $r = |\vec{r}|$ is the distance from the center of the nucleus, and m is the reduced mass of the h -nucleus system in vacuum, with $h = \eta, \eta'$. In this case the bound state energies (E) of the h -nucleus system are given by $E = \mathcal{E} - m$, where \mathcal{E} is the energy eigenvalue in Eq. (13).

For the solution of Eqs. (12) and (13), we use momentum space methods. Here these equations are first converted to a momentum space representation via a Fourier transform, followed by a partial wave decomposition of the Fourier-transformed potential. Then for a given value of angular momentum (ℓ), the eigenvalues of the resulting equation are found by the inverse iteration eigenvalue algorithm. We note

TABLE II. Bound state energies (E) of the η' meson in nucleus of mass number A obtained by solving the Schrödinger and Klein-Gordon equations. E is in MeV.

	$n\ell$	E (SE)	E (KGE)
${}^4_{\eta'}\text{He}$	1s	-23.72	-22.11
${}^{12}_{\eta'}\text{C}$	1s	-34.79	-33.88
	1p	-13.63	-12.72
${}^{16}_{\eta'}\text{O}$	1s	-39.47	-38.64
	1p	-20.81	-19.75
${}^{40}_{\eta'}\text{Ca}$	2s	-1.88	-1.39
	1d	-1.76	-0.33
	1s	-53.09	-52.38
	1p	-39.52	-38.41
${}^{48}_{\eta'}\text{Ca}$	1d	-24.41	-23.12
	2s	-21.66	-20.38
	1s	-53.01	-52.40
	1p	-41.29	-40.30
${}^{90}_{\eta'}\text{Zr}$	1d	-27.90	-26.68
	2s	-24.69	-23.45
	1s	-55.62	-55.20
	1p	-47.79	-47.05
${}^{197}_{\eta'}\text{Au}$	1d	-38.47	-37.42
	2s	-35.31	-34.19
	1s	-56.28	-56.03
	1p	-51.59	-51.12
${}^{208}_{\eta'}\text{Pb}$	1d	-45.87	-45.15
	2s	-43.60	-42.80
	1s	-57.90	-57.65
	1p	-53.26	-52.77
	1d	-47.60	-46.87
	2s	-45.38	-44.56

that at this point there is no advantage in using momentum space methods. However, the advantage will be apparent later, when we add an imaginary part to the nuclear potential, in order to simulate absorption of the η and η' mesons by nuclei.

The results obtained for the single-particle energies E for the η and η' are listed in Tables I and II, respectively, for all nuclei listed in the previous section. In Table I we show the η -nucleus bound state energies obtained by solving the Schrödinger and Klein-Gordon equations. For each nucleus we have computed all bound states but have listed only a few of them (up to four). However, we note that the number of bound states increases with the mass of the nucleus, such that for the heavier nuclei we have a richer structure of bound states. Furthermore, we note that the relativistic corrections decrease the bound state energies for the η by approximately 2 MeV.

In Table II we show the η' -nucleus bound state energies obtained by solving the Schrödinger and Klein-Gordon equations. As in the η case, for each nucleus we have listed up to four bound states. We see that compared to the η meson, for the η' we have a richer structure of bound states due to the fact that the η' is heavier. Finally, we note that the relativistic corrections are smaller for the η' meson, by approximately 1 MeV, due to its larger mass. Thus from Tables I and II we conclude that the η and η' are expected to form mesic nuclei

TABLE III. Bound state energies (E) and full widths (Γ) of η meson in nucleus of mass number A obtained by solving the Schrödinger for various values of γ .

	$n\ell$	$\gamma = 0$		$\gamma = 0.25$		$\gamma = 0.5$		$\gamma = 1.0$	
		E	Γ	E	Γ	E	Γ	E	Γ
${}^4_\eta\text{He}$	1s	-13.24	0	-12.97	9.81	-12.21	19.86	-9.45	41.45
${}^{12}_\eta\text{C}$	1s	-27.03	0	-26.92	11.77	-26.60	23.64	-25.44	47.97
	1p	-1.75	0	-1.33	6.05	N	N	N	N
${}^{16}_\eta\text{O}$	1s	-32.60	0	-32.51	12.84	-32.27	25.77	-31.39	52.09
	1p	-8.04	0	-7.80	8.99	-7.12	18.30	-4.84	38.46
${}^{40}_\eta\text{Ca}$	1s	-48.71	0	-48.66	15.86	-48.52	31.76	-48.00	63.84
	1p	-29.31	0	-29.20	13.83	-28.88	27.78	-27.75	56.30
	1d	-8.73	0	-8.50	10.92	-7.84	22.14	-5.64	46.09
${}^{48}_\eta\text{Ca}$	2s	-7.16	0	-6.79	9.01	-5.77	18.56	N	N
	1s	-49.34	0	-49.31	15.61	-49.19	31.25	-48.78	62.77
	1p	-32.22	0	-32.13	14.03	-31.88	28.15	-30.97	56.91
	1d	-13.31	0	-13.13	11.80	-12.63	23.81	-10.90	48.98
${}^{90}_\eta\text{Zr}$	2s	-10.34	0	-10.05	10.25	-9.26	20.91	N	N
	1s	-53.71	0	-53.69	15.77	-53.63	31.56	-53.40	63.27
	1p	-41.76	0	-41.71	14.95	-41.57	29.94	-41.08	60.22
	1d	-27.71	0	-27.62	13.85	-27.36	27.79	-26.49	56.21
${}^{197}_\eta\text{Au}$	2s	-23.43	0	-22.28	9.68	-22.95	26.47	-21.75	53.93
	1s	-55.85	0	-55.84	15.45	-55.81	30.92	-55.69	61.91
	1p	-48.45	0	-48.43	15.07	-48.36	30.16	-48.13	60.47
	1d	-39.48	0	-39.44	14.56	-39.32	29.17	-38.91	58.62
${}^{208}_\eta\text{Pb}$	2s	-36.04	0	-35.99	14.29	-35.84	28.63	-35.31	57.66
	1s	-57.59	0	-57.58	15.87	-57.55	31.76	-57.44	63.58
	1p	-50.27	0	-50.25	15.49	-50.18	30.99	-49.95	62.14
	1d	-41.40	0	-41.36	14.99	-41.25	30.01	-40.85	60.30
	2s	-38.03	0	-37.98	14.72	-37.83	29.50	-37.32	59.37

with all the nuclei considered. However, this is not a definite conclusion, since so far we have not taken into account the absorption of these mesons by nuclei.

V. SINGLE-PARTICLE ENERGIES AND ABSORPTION WIDTHS FOR THE η AND η' IN NUCLEI.

In order to make our results more realistic, we now add an important feature of the meson-nucleus interaction that was neglected in Ref. [34] for the η' , namely, meson absorption in nuclei, which requires a complex potential. We follow Refs. [33,34] and construct this potential phenomenologically by adding an imaginary part $W_{hA}(r)$ to the η and η' scalar potentials discussed in the previous section, given in Eq. (11), as follows:

$$V_{hA}(r) = \Delta m_h(\rho_B^A(r)) + iW_{hA}(r), \quad (14)$$

where $W_{hA}(r)$ is related to the absorption of the meson h in the nuclear medium and is given by

$$W_{hA}(r) = -\frac{1}{2}\Gamma_{hA}(r), \quad (15)$$

$$\Gamma_{hA}(r) = -\gamma\Delta m_h(\rho_B^A(r)) + \Gamma_h^{\text{vac}}. \quad (16)$$

Here Γ_h^{vac} is the meson decay width in vacuum ($\Gamma_\eta^{\text{vac}} = 1.31$ keV and $\Gamma_{\eta'}^{\text{vac}} = 0.188$ MeV [40]), and γ is a phenomenological parameter used to simulate the strength of the absorption of the meson in the nuclear medium.

Next we calculate the bound state energies and widths for the η - and η' -mesic nuclei using the Schrödinger and Klein-Gordon equations with the complex potential, Eq. (14), for several values of the parameter γ , which cover the estimated widths of the η and η' mesons in the nuclear medium quoted in the Introduction section.

For the moment we ignore Γ_h^{vac} ; however, since it is very small it will not contribute much. In Tables III and IV we show the results for the bound state energies (E) and full widths (Γ) of the η -mesic nuclei of mass number A , obtained by solving the Schrödinger and Klein-Gordon equations, respectively, for various values of the strength of the imaginary part of the potential $\gamma = 0.0, 0.25, 0.5, 1.0$. The bound state energies and full widths are obtained from the complex energy eigenvalue \mathcal{E} as $\mathcal{E} = E - i\Gamma/2$ for the Schrödinger equation and as $\mathcal{E} = E + m - i\Gamma/2$ for the Klein-Gordon equation. In Tables V and VI we present the corresponding results for the η' meson. Note that the results for $\gamma = 0$, for both the η and η' mesons, correspond to the results given in Tables I and II, which we have already discussed in the previous section.

We now discuss the results obtained when the imaginary part of the potential is included, columns with $\gamma = 0.25, 0.5$ and $\gamma = 1.0$ in Tables III–VI. The following conclusions, obtained from Tables III–VI, apply both to the η - and η' -mesic nuclei. For now we will only discuss the ground states, since all mesic nuclei have at least one bound state.

TABLE IV. Bound state energies (E) and full widths (Γ) of η meson in nucleus of mass number A obtained by solving the Klein-Gordon equation for various values of γ .

	$n\ell$	$\gamma = 0$		$\gamma = 0.25$		$\gamma = 0.5$		$\gamma = 1.0$	
		E	Γ	E	Γ	E	Γ	E	Γ
${}^4_\eta\text{He}$	1s	-10.99	0	-10.79	8.21	-10.20	16.65	-8.13	34.94
${}^{12}_\eta\text{C}$	1s	-25.25	0	-25.16	10.86	-24.91	21.82	-24.02	44.29
	1p	-0.87	0	-0.43	4.97	N	N	N	N
${}^{16}_\eta\text{O}$	1s	-30.78	0	-30.72	12.00	-30.53	24.07	-29.86	48.67
	1p	-6.47	0	-6.26	7.84	-5.67	15.99	-3.77	33.80
${}^{40}_\eta\text{Ca}$	1s	-46.93	0	-46.89	15.12	-46.79	30.28	-46.43	60.87
	1p	-26.93	0	-26.85	12.67	-26.61	25.44	-25.77	51.59
	1d	-6.67	0	-6.47	9.48	-5.91	19.27	-4.15	40.31
${}^{48}_\eta\text{Ca}$	2s	-5.43	0	-5.09	7.51	-4.18	15.59	N	N
	1s	-47.78	0	-47.75	14.98	-47.66	30.00	-47.38	60.25
	1p	-29.97	0	-29.90	12.99	-29.71	26.06	-29.04	52.71
	1d	-11.08	0	-10.93	10.45	-10.51	21.10	-9.15	43.52
${}^{90}_\eta\text{Zr}$	2s	-8.7	0	-8.11	8.83	-7.42	18.06	N	N
	1s	-52.56	0	-52.54	15.34	-52.50	30.71	-52.34	61.56
	1p	-39.85	0	-39.81	14.17	-39.71	28.40	-39.36	57.11
	1d	-25.32	0	-25.25	12.74	-25.06	25.57	-24.40	51.75
${}^{197}_\eta\text{Au}$	2s	-21.04	0	-20.94	11.95	-20.65	24.04	-19.70	49.03
	1s	-55.12	0	-55.11	15.20	-55.09	30.41	-55.01	60.89
	1p	-47.13	0	-47.11	14.58	-47.06	29.19	-46.90	58.53
	1d	-37.60	0	-37.58	13.83	-37.49	27.69	-37.20	55.67
${}^{208}_\eta\text{Pb}$	2s	-34.01	0	-33.97	13.45	-33.86	26.96	-33.47	54.31
	1s	-56.85	0	-56.84	15.61	-56.82	31.24	-56.75	62.55
	1p	-48.92	0	-48.90	14.99	-48.86	30.01	-48.70	60.17
	1d	-39.81	0	-39.45	14.24	-39.37	28.51	-39.09	57.29
	2s	-35.95	0	-35.91	13.87	-35.80	27.80	-35.43	55.96

Adding an absorptive part of the potential changes the situation appreciably. The effects are larger the larger γ is for both the nonrelativistic and relativistic cases. Clearly, the imaginary part of the potential is repulsive, being more repulsive for $\gamma = 1$. Whether or not the bound states can be observed experimentally is sensitive to the value of the parameter γ , since Γ increases with increasing γ . Furthermore, since the so-called dispersive effect of the absorptive potential is repulsive, the binding energies for all nuclei decrease with γ . However, they decrease very little. Even for the largest value of γ , there is at least one bound state. We have found similar results for the ϕ meson in a previous paper [36]. Note that the width of the ground state increases with γ for all nuclei, as expected, since a larger γ means that the strength of the imaginary part of the potential is larger.

η - and η' -mesic bound states have been studied by several authors in a variety of approaches, such as the QMC model [9,22], chiral coupled channels [23], the Nambu–Jona-Lasinio model [24–26], and linear σ model [27,28], and chiral unitary approach using a microscopic many-body theory [29,30], as well as other more formal approaches [31,32]. It is interesting to compare our results with those of Refs. [29,30], where both real and imaginary parts of the potential have been evaluated from the η self-energy in nuclei in chiral unitary approach. For the nuclei for which the comparison is possible (${}^{12}_\eta\text{C}$, ${}^{40}_\eta\text{Ca}$,

and ${}^{208}_\eta\text{Pb}$), we see that our bound state energies are more than twice theirs (see Table 1 Ref. [29]) when we compare with their results obtained using an energy-dependent potential; however, the situation improves to our favor when we compare with their results obtained using an energy-independent potential. The fact that our results compare better with those of Ref. [29] seems to indicate that we can improve our results, and reduce the amount of binding energy, by taking into account the energy and momentum dependence of the η (and η') self-energy. The main goal of the present work is to improve the previous results by adding an imaginary part to the potential in order to assess the feasibility of observation of the η - and η' -mesic nuclei predicted by our approach. In any case, it is possible that our results give overbinding. This may be based on the results from Ref. [50], where no clear ${}^4_\eta\text{He}$ bound states are found. The analysis in Ref. [50] is carried by analyzing the data on the cross section for the $dd \rightarrow \eta^4\text{He}$ reaction close to threshold. However, the present approach is based on the mean-field approach, and then the results for lighter nuclei may not be appropriate for ${}^4_\eta\text{He}$. In fact, the nucleon density distribution for ${}^4\text{He}$ is not calculated here, which is the basis to calculate the ${}^4_\eta\text{He}$ potential. Furthermore, in the case when the width of the η (imaginary part of the potential) is indeed large in reality, the conclusion drawn based on the experimental data that they found no bound η -nucleus states may be changed. That is why we have addressed the

TABLE V. Bound state energies (E) and full widths (Γ) of η' meson in nucleus of mass number A obtained by solving the Schrödinger equation for various values of γ .

	$n\ell$	$\gamma = 0$		$\gamma = 0.25$		$\gamma = 0.5$		$\gamma = 1.0$	
		E	Γ	E	Γ	E	Γ	E	Γ
${}^4_{\eta'}\text{He}$	1s	-23.72	0	-23.55	12.27	-23.06	24.70	-21.29	50.50
${}^{12}_{\eta'}\text{C}$	1s	-34.79	0	-34.72	12.70	-34.52	25.47	-33.78	51.37
	1p	-13.63	0	-13.47	9.62	-13.00	19.41	-11.35	39.95
${}^{16}_{\eta'}\text{O}$	1s	-39.47	0	-39.42	13.40	-39.27	26.86	-38.74	54.04
	1p	-20.81	0	-20.69	11.31	-20.35	22.73	-19.16	46.28
	2s	-1.88	0	-1.33	5.22	N	N	N	N
${}^{40}_{\eta'}\text{Ca}$	1d	-1.76	0	-1.43	7.89	-0.35	13.61	N	N
	1s	-53.09	0	-53.06	15.87	-52.98	31.76	-52.66	63.71
	1p	-39.52	0	-39.45	14.65	-39.27	29.35	-38.62	59.11
${}^{48}_{\eta'}\text{Ca}$	1d	-24.41	0	-24.30	13.10	-23.98	26.31	-22.85	53.40
	2s	-21.66	0	-21.51	12.40	-21.09	24.96	-19.64	51.01
	1s	-53.01	0	-52.99	15.5	-52.92	31.05	-52.67	62.25
${}^{90}_{\eta'}\text{Zr}$	1p	-41.29	0	-41.24	14.58	-41.10	29.20	-40.58	58.73
	1d	-27.90	0	-27.81	13.38	-27.56	26.85	-26.67	54.32
	2s	-24.69	0	-24.57	12.81	-24.24	25.74	-23.09	52.33
${}^{90}_{\eta'}\text{Zr}$	1s	-55.62	0	-55.61	15.45	-55.57	30.92	-55.44	61.92
	1p	-47.79	0	-47.77	14.98	-47.69	29.98	-47.42	60.13
	1d	-38.47	0	-38.42	14.37	-38.29	28.78	-37.82	57.88
${}^{197}_{\eta'}\text{Au}$	2s	-35.31	0	-35.25	14.07	-35.08	28.21	-34.49	56.84
	1s	-56.28	0	-56.28	15.03	-56.26	30.06	-56.20	60.15
	1p	-51.59	0	-51.58	14.80	-51.54	29.61	-51.41	59.31
${}^{197}_{\eta'}\text{Au}$	1d	-45.87	0	-45.85	14.52	-45.79	29.06	-45.57	58.26
	2s	-43.60	0	-43.57	14.39	-43.50	28.80	-43.02	58.09
	1s	-57.90	0	-57.90	15.42	-57.88	30.84	-57.81	61.73
${}^{208}_{\eta'}\text{Pb}$	1p	-53.26	0	-53.24	15.19	-53.21	30.40	-53.08	60.88
	1d	-47.60	0	-47.57	14.91	-47.51	29.84	-47.29	59.83
	2s	-45.38	0	-45.35	14.78	-45.27	29.59	-45.01	59.36

calculation with a wider range of the imaginary part of the potential.

VI. SUMMARY AND CONCLUSIONS

We have updated the mass shift of the η and η' mesons in symmetric nuclear matter using the most up to date mixing angle, $\theta_p = -11.3^\circ$, within the quark-meson coupling model. Using these mass shift as input, we have calculated, in the local density approximation, the real part of the scalar nuclear potential for the η and η' mesons for various nuclei, covering a wide range of nuclear masses. The nuclear density distributions for all nuclei, except the lightest one, were computed using the quark-meson coupling model self-consistently. We found that these potentials are attractive in all cases. Then we calculated the bound state energies for the η - and η' -mesic nuclei for several nuclei by solving the Schrödinger and Klein-Gordon equations. We found that by neglecting meson absorption by nuclei, these mesons should form mesic nuclei with all the nuclei considered. Even though this is an important step, it ignores the absorption of these mesons by nuclei. To remedy this, we have added, in a phenomenological way, an imaginary part to the η - and η' -nucleus potentials with wider ranges and again solved the Schrödinger and Klein-Gordon equations with complex

potentials. Our results show that the η and η' mesons are expected to form mesic nuclei with all the nuclei considered. The main feature of forming bound states with nuclei is not changed by the introduction of imaginary parts of the potentials, though the feasibility for experiment is certainly influenced. Namely, the signal for the formation of the η - and η' -mesic nuclei may be difficult to identify experimentally, given the similarity between the real and imaginary parts (widths) of the bound state energies. Furthermore, our results depend on the strength of the imaginary part of the meson-nucleus potential, as expected. Thus, in order to quantify this uncertainty and the sensitivity of our results to its value, we have analyzed three values of strength for the imaginary part of the meson-nucleus potential. Therefore the feasibility of observation of the η - and η' -mesic nuclei needs further investigation.

ACKNOWLEDGMENTS

The authors acknowledge the support and warm hospitality of APCTP (Asia Pacific Center for Theoretical Physics), as they hosted a workshop where part of the present work was presented and discussed. The authors also thank the OMEG (Origin of Matter and Evolution of Galaxies) Institute at Soongsil University for support during the collaboration

TABLE VI. Bound state energies (E) and full widths (Γ) of η' meson in nucleus of mass number A obtained by solving the Klein-Gordon equation for various values of γ .

	$n\ell$	$\gamma = 0$		$\gamma = 0.25$		$\gamma = 0.5$		$\gamma = 1.0$	
		E	Γ	E	Γ	E	Γ	E	Γ
${}^4_{\eta'}$ He	1s	-22.11	0	-21.96	11.37	-21.55	22.89	-20.06	46.83
${}^{12}_{\eta'}$ C	1s	-33.88	0	-33.82	12.30	-33.64	24.66	-33.00	49.73
	1p	-12.72	0	-12.57	9.06	-12.15	18.29	-10.67	37.68
${}^{16}_{\eta'}$ O	1s	-38.64	0	-38.59	13.06	-38.46	26.17	-38.00	52.65
	1p	-19.75	0	-19.65	10.76	-19.34	21.64	-18.28	44.07
	2s	-1.39	0	-0.84	4.48	N	N	N	N
	1d	-0.33	0	-0.69	7.20	N	N	N	N
${}^{40}_{\eta'}$ Ca	1s	-52.38	0	-52.35	15.59	-52.28	31.22	-52.00	62.61
	1p	-38.41	0	-38.35	14.18	-38.19	28.41	-37.63	57.22
	1d	-23.12	0	-23.02	12.46	-22.74	25.03	-21.75	50.81
	2s	-20.38	0	-20.25	11.72	-19.87	23.60	-18.58	48.25
${}^{48}_{\eta'}$ Ca	1s	-52.40	0	-52.38	15.29	-52.32	30.60	-52.11	61.35
	1p	-40.30	0	-40.26	14.18	-40.13	28.40	-39.68	57.12
	1d	-26.68	0	-26.59	12.82	-26.37	25.72	-25.58	52.02
	2s	-23.45	0	-23.34	12.19	-23.04	24.51	-22.01	49.85
${}^{90}_{\eta'}$ Zr	1s	-55.20	0	-55.19	15.31	-55.16	30.63	-55.04	61.35
	1p	-47.05	0	-47.02	14.70	-46.96	29.43	-46.72	59.04
	1d	-37.42	0	-37.38	13.96	-37.27	27.96	-36.86	56.22
	2s	-34.19	0	-34.14	13.61	-33.99	27.29	-33.47	54.98
${}^{197}_{\eta'}$ Au	1s	-56.03	0	-56.03	14.94	-56.01	29.89	-55.96	59.83
	1p	-51.12	0	-51.10	14.64	-51.07	29.30	-50.96	58.67
	1d	-45.15	0	-45.14	14.27	-45.08	28.56	-44.89	57.26
	2s	-42.80	0	-42.78	14.10	-42.71	28.22	-42.47	56.63
${}^{208}_{\eta'}$ Pb	1s	-57.65	0	-57.64	15.34	-57.63	30.68	-57.57	61.40
	1p	-52.77	0	-52.76	15.03	-52.73	30.07	-52.62	60.23
	1d	-46.87	0	-46.85	14.66	-46.80	29.33	-46.61	58.80
	2s	-44.56	0	-44.54	14.49	-44.47	29.00	-44.24	58.19

visit in Korea. J.J.C.-M. acknowledges financial support from the University of Sonora under Grant No. USO315007861. K.T. was supported by Conselho Nacional de Desenvolvimento Científico e Tecnológico (CNPq, Brazil), Processes No. 313063/2018-4 and No. 426150/2018-0, and FAPESP

Processes No. 2019/00763-0 and No. 2023/07313-6. This work was also funded by Instituto Nacional de Ciência e Tecnologia - Nuclear Physics and Applications (INCT-FNA), Brazil, through Process No. 464898/2014-5, and FAPESP Temático, Brazil, through Process No. 2017/05660-0.

- [1] T. Nishi *et al.* (piAF Collaboration), Chiral symmetry restoration at high matter density observed in pionic atoms, *Nat. Phys.* **19**, 788 (2023).
- [2] G. Krein, A. W. Thomas and K. Tsushima, Nuclear-bound quarkonia and heavy-flavor hadrons, *Prog. Part. Nucl. Phys.* **100**, 161 (2018).
- [3] V. Metag, M. Nanova, and E. Y. Paryev, Meson–nucleus potentials and the search for meson–nucleus bound states, *Prog. Part. Nucl. Phys.* **97**, 199 (2017).
- [4] A. Khreptak, M. Skurzok, and P. Moskal, Search for η -mesic nuclei: A review of experimental and theoretical advances, *Front. Phys.* **11**, 1186457 (2023).
- [5] S. D. Bass, V. Metag, and P. Moskal, The η - and η' -nucleus interactions and the search for η , η' -mesic states, in *Handbook of Nuclear Physics*, edited by I. Tanihata, H. Toki, and T. Kajino (Springer, Singapore, 2022).
- [6] Q. Haider and L. C. Liu, Eta-mesic nuclei: Past, present, future, *Int. J. Mod. Phys. E* **24**, 1530009 (2015).
- [7] S. D. Bass and P. Moskal, η' and η mesons with connection to anomalous glue, *Rev. Mod. Phys.* **91**, 015003 (2019).
- [8] N. G. Kelkar, K. P. Khemchandani, N. J. Upadhyay and B. K. Jain, Interaction of η mesons with nuclei, *Rep. Prog. Phys.* **76**, 066301 (2013).
- [9] S. D. Bass and A. W. Thomas, Eta bound states in nuclei: A probe of flavor-singlet dynamics, *Phys. Lett. B* **634**, 368 (2006).
- [10] J. Li, J. Gui, and P. Zhuang, $U_A(1)$ symmetry restoration at high baryon density, *Chin. Phys. C* **47**, 104102 (2023).
- [11] Q. Haider and L. C. Liu, Formation of an η mesic nucleus, *Phys. Lett. B* **172**, 257 (1986).
- [12] M. Skurzok, P. Moskal, N. G. Kelkar, S. Hirenzaki, H. Nagahiro, and N. Ikeno, Constraining the optical potential in the search for η -mesic ${}^4\text{He}$, *Phys. Lett. B* **782**, 6 (2018).
- [13] N. Ikeno, H. Nagahiro, D. Jido, and S. Hirenzaki, η -nucleus interaction from the $d + d$ reaction around the η production threshold, *Eur. Phys. J. A* **53**, 194 (2017).

- [14] M. Nanova *et al.* (CBELSA/TAPS Collaboration), Determination of the real part of the η' -Nb optical potential, *Phys. Rev. C* **94**, 025205 (2016).
- [15] M. Nanova *et al.* (CBELSA/TAPS Collaboration), Determination of the η' -nucleus optical potential, *Phys. Lett. B* **727**, 417 (2013).
- [16] M. Nanova *et al.* (CBELSA/TAPS Collaboration), The η' -carbon potential at low meson momenta, *Eur. Phys. J. A* **54**, 182 (2018).
- [17] M. Nanova *et al.* (CBELSA/TAPS Collaboration), Transparency ratio in $\gamma A \rightarrow \eta' A'$ and the in-medium η' width, *Phys. Lett. B* **710**, 600 (2012).
- [18] S. Friedrich *et al.* (CBELSA/TAPS Collaboration), Momentum dependence of the imaginary part of the ω - and η' -nucleus optical potential, *Eur. Phys. J. A* **52**, 297 (2016).
- [19] N. Tomida *et al.* (LEPS2/BGOegg Collaboration), Search for η' bound nuclei in the $^{12}\text{C}(\gamma, p)$ reaction with simultaneous detection of decay products, *Phys. Rev. Lett.* **124**, 202501 (2020).
- [20] H. Fujioka, K. Itahashi, V. Metag, M. Nanova and Y. K. Tanaka, Comment on search for η' bound nuclei in the $^{12}\text{C}(\gamma, p)$ reaction with simultaneous detection of decay products, *Phys. Rev. Lett.* **126**, 019201 (2021).
- [21] Y. K. Tanaka *et al.* (n-PRiME/Super-FRS Collaboration), Measurement of excitation spectra in the $^{12}\text{C}(p, d)$ reaction near the η' emission threshold, *Phys. Rev. Lett.* **117**, 202501 (2016).
- [22] S. D. Bass and A. W. Thomas, QCD Symmetries in η - and η' -mesic nuclei, *Acta Phys. Pol. B* **45**, 627 (2014).
- [23] H. Nagahiro, S. Hirenzaki, E. Oset, and A. Ramos, η' -nucleus optical potential and possible η' -bound states, *Phys. Lett. B* **709**, 87 (2012).
- [24] V. Bernard and U. G. Meissner, Meson properties at finite density from $\text{SU}(3)_f$ quark dynamics, *Phys. Rev. D* **38**, 1551 (1988).
- [25] H. Nagahiro, M. Takizawa and S. Hirenzaki, η - and η' -mesic nuclei and $\text{U}(A)(1)$ anomaly at finite density, *Phys. Rev. C* **74**, 045203 (2006).
- [26] P. Costa, M. C. Ruivo, and Y. L. Kalinovsky, Pseudoscalar neutral mesons in hot and dense matter, *Phys. Lett. B* **560**, 171 (2003).
- [27] S. Sakai and D. Jido, In-medium η' mass and $\eta'N$ interaction based on chiral effective theory, *Phys. Rev. C* **88**, 064906 (2013).
- [28] S. Sakai and D. Jido, Spectral function of the η' meson in nuclear medium based on phenomenological models, *Phys. Rev. C* **107**, 025207 (2023).
- [29] C. García-Recio, J. Nieves, T. Inoue and E. Oset, η bound states in nuclei, *Phys. Lett. B* **550**, 47 (2002).
- [30] T. Inoue and E. Oset, η in the nuclear medium within a chiral unitary approach, *Nucl. Phys. A* **710**, 354 (2002).
- [31] D. Jido, H. Nagahiro, and S. Hirenzaki, Nuclear bound state of $\eta'(958)$ and partial restoration of chiral symmetry in the η' mass, *Phys. Rev. C* **85**, 032201(R) (2012).
- [32] H. Nagahiro and S. Hirenzaki, Formation of $\eta'(958)$ -mesic nuclei and axial $\text{U}(A)(1)$ anomaly at finite density, *Phys. Rev. Lett.* **94**, 232503 (2005).
- [33] K. Tsushima, D. H. Lu, A. W. Thomas, and K. Saito, Are η and ω nuclear states bound? *Phys. Lett. B* **443**, 26 (1998).
- [34] K. Tsushima, Study of ω -, η -, η' - and D^- -mesic nuclei, *Nucl. Phys. A* **670**, 198 (2000).
- [35] J. J. Cobos-Martínez, K. Tsushima, G. Krein and A. W. Thomas, ϕ meson mass and decay width in nuclear matter and nuclei, *Phys. Lett. B* **771**, 113 (2017).
- [36] J. J. Cobos-Martínez, K. Tsushima, G. Krein, and A. W. Thomas, Φ -meson-nucleus bound states, *Phys. Rev. C* **96**, 035201 (2017).
- [37] J. J. Cobos-Martínez, K. Tsushima, G. Krein and A. W. Thomas, η_c -nucleus bound states, *Phys. Lett. B* **811**, 135882 (2020).
- [38] G. N. Zeminiani, J. J. Cobos-Martínez, and K. Tsushima, Υ and η_b mass shifts in nuclear matter, *Eur. Phys. J. A* **57**, 259 (2021).
- [39] J. J. Cobos-Martínez, G. N. Zeminiani, and K. Tsushima, Υ and η_b nuclear bound states, *Phys. Rev. C* **105**, 025204 (2022).
- [40] R. L. Workman *et al.* (Particle Data Group Collaboration), Review of particle physics, *PTEP* **2022**, 083C01 (2022).
- [41] P. A. M. Guichon, A possible quark mechanism for the saturation of nuclear matter, *Phys. Lett. B* **200**, 235 (1988).
- [42] K. Saito, K. Tsushima and A. W. Thomas, Nucleon and hadron structure changes in the nuclear medium and impact on observables, *Prog. Part. Nucl. Phys.* **58**, 1 (2007).
- [43] P. A. M. Guichon, J. R. Stone and A. W. Thomas, Quark-meson-coupling (QMC) model for finite nuclei, nuclear matter and beyond, *Prog. Part. Nucl. Phys.* **100**, 262 (2018).
- [44] K. Tsushima, K. Saito, A. W. Thomas, and S. V. Wright, In-medium kaon and antikaon properties in the quark-meson coupling model, *Phys. Lett. B* **429**, 239 (1998); Erratum, **436**, 453 (1998).
- [45] P. A. M. Guichon, K. Saito, E. N. Rodionov and A. W. Thomas, The role of nucleon structure in finite nuclei, *Nucl. Phys. A* **601**, 349 (1996).
- [46] K. Tsushima, Magnetic moments of the octet, decuplet, low-lying charm, and low-lying bottom baryons in a nuclear medium, *PTEP* **2022**, 043D02 (2022).
- [47] T. Feldmann, Quark structure of pseudoscalar mesons, *Int. J. Mod. Phys. A* **15**, 159 (2000).
- [48] K. Saito, K. Tsushima and A. W. Thomas, Self-consistent description of finite nuclei based on a relativistic quark model, *Nucl. Phys. A* **609**, 339 (1996).
- [49] K. Saito, K. Tsushima and A. W. Thomas, Rho meson mass in light nuclei, *Phys. Rev. C* **56**, 566 (1997).
- [50] J. J. Xie, W. H. Liang, and E. Oset, η - ^4He interaction from the $dd \rightarrow \eta^4\text{He}$ reaction near threshold, *Eur. Phys. J. A* **55**, 6 (2019).